Molecular Structure of Magnesium Dibromide: An Electron Diffraction and Quantum Chemical Study

Balázs Réffy, Mária Kolonits, and Magdolna Hargittai*

Structural Chemistry Research Group of the Hungarian Academy of Sciences at Eötvös University, P.O. Box 32, H-1518 Budapest, Hungary

Received: June 8, 2005

The molecular structure of magnesium dibromide was investigated by high-level computational techniques and gas-phase electron diffraction. The vapor consisted of about 88% monomeric and 12% dimeric species at the electron diffraction experimental conditions at 1065 K. The geometrical parameters and vibrational characteristics of monomeric, dimeric, and trimeric magnesium dibromide species were determined by computations. Very high level computations with extended basis sets and relativistic pseudopotentials on bromine were needed to reach an agreement between computed and estimated experimental equilibrium geometries for the monomer. For both the dimer and the trimer, different geometrical arrangements were tested. Their ground-state structures have halogen bridges with four-membered ring geometries and D_{2h} and D_{2d} symmetry, respectively. Thermodynamic parameters have also been calculated.

Introduction

Magnesium dibromide is best known in connection with the widely used Grignard reagent in organic syntheses.[1] The so-called Schlenk equilibrium[2] describes the process, in which the associated species can be dimers, trimers, and even larger associates may be involved. Magnesium dibromide crystallizes in a CdI_2-type layer structure,[3] although recently a high-temperature polymorphic modification was also found, which crystallizes in the $CdCl_2$-type structure.[4] The gas-phase monomeric molecule was studied in the early days of the gas-electron diffraction (GED) technique by the so-called visual method, and its bond length was estimated.[5] Simple as the composition of such a molecule is, there are many pitfalls in its structure determination. The vapor composition of magnesium dibromide may be rather complex, and this was ignored in the early study. Further complication is the high experimental temperature and the anharmonicity of the vibrations associated with these types of molecules.[6] The gas-phase IR spectrum of magnesium dibromide was studied by Randall et al.,[7] the matrix isolation IR spectra by Cocke et al.,[8] and both the matrix isolation IR and Raman spectra by Lesiecki and Nibler.[9] Besides determining the frequencies and shape of the monomer, they also measured frequencies that could be attributed to dimeric molecules. Even the possibility of the presence of some trimers could not be excluded. The vapors of alkaline earth dihalides have been shown to contain small oligomers in addition to monomeric molecules,[10] and the tendency to contain larger species seems to be strongest for the halides of magnesium. The electron diffraction study of magnesium dichloride detected about 13% of dimers in the vapor.[11] On the other hand, an early mass spectrometric study of all magnesium dihalides detected only an about 1% dimeric species in their vapors[12] alas at a few hundred degrees lower temperature than the temperature of the GED experiments. As it will be discussed, such a difference in the experimental temperatures seriously influences the vapor content. The vapors of calcium dihalides have been shown to have less than 5% dimeric species in their vapor by electron diffraction,[13] and there were no measurable amounts of dimers in the vapors of the strontium[14] and barium dibromides.[15] Computational studies of magnesium dibromide include the comprehensive studies of alkaline earth dihalides by Seijo and Barandiarán,[16] Knaupp et al.,[17] and Axten et al.[18] The latter also determined the structure of the dimer but only at the Hartree−Fock (HF) level.

The lack of reliable experimental data on the geometrical parameters of magnesium dibromide prompted us to determine its structure by electron diffraction. At the same time, we also carried out high-level computational studies of the monomers, dimers, and trimers of this molecule and determined their structures and some of their thermodynamic functions.

Experimental Section

Magnesium dibromide was prepared by D. Knausz of Eötvös University from magnesium metal and bromine.[19] Its purity was checked by mass spectrometry. The sample was evaporated in our combined electron-diffraction quadrupole mass spectrometric experiment developed in the Budapest laboratory,[20] with a modified EG-100A apparatus[21] and with a radiation-type nozzle system and a molybdenum nozzle. The experimental temperature was 1065 K, and the accelerating voltage was 60 kV. The mass spectra indicated the presence of monomeric and also other species in the vapor. Four and five photographic plates were used in the analysis taken at 50 and 19 cm camera ranges, respectively. The data intervals were 2.50−14.00 $Å^{-1}$ (with 0.125 $Å^{-1}$ steps) and 9.00−30.00 $Å^{-1}$ (with 0.25 $Å^{-1}$ steps) at the two camera ranges, respectively. Electron scattering factors were taken from the literature.[22] Listings of electron diffraction molecular intensities are given in the Supporting Information. The molecular intensity and radial distribution curves are shown in Figures 1 and 2.

Quantum-Chemical Calculations. Quantum-chemical calculations were performed at different levels of theory and used

* To whom correspondence should be addressed. E-mail: hargitta@ludens.elte.hu.

10.1021/jp0530606 CCC: $30.25
Published on Web 08/30/2005

TABLE 1: Geometrical Parameters of $MgBr_2$ and Mg_2Br_4 from Computation (distances in Å, angles in degrees)

	basis[a]		$MgBr_2$	Mg_2Br_4				
method	Mg	Br	Mg−Br	Mg−Br_t	Mg−Br_b	Br_b−Mg−Br_b	$\Delta(D_t - \text{mon})$[b]	$\Delta(D_b - D_t)$[c]
B3LYP	TZ	SDB−TZ	2.326	2.335	2.523	95.8	0.009	0.188
MP2			2.326	2.332	2.513	95.6	0.006	0.181
B3LYP	ATZ	SDB−TZ	2.328	2.337	2.522	95.8	0.009	0.185
MP2			2.329	2.335	2.513	95.6	0.006	0.178
MP2	ATZ	SDB−ATZ	2.330	2.337	2.516	95.5	0.007	0.179
MP2	TZ	TZ−PP	2.318					
CCSD(T)			2.321					
MP2	QZ	QZ	2.319					
CCSD(T)			2.324					
MP2	QZ	SDB−QZ	2.325					
CCSD(T)			2.326					
MP2	5Z	SDB−QZ	2.321					
CCSD(T)			2.323					
MP2	QZ	QZ−PP	2.311	2.319	2.495	95.3	0.008	0.176
CCSD(T)			2.314					
MP2	AQZ	AQZ−PP	2.311					
MP2	CQZ	QZ−PP	2.307					
CCSD(T)			2.310					
MP2	CQZ	AQZ−PP	2.308					
MP2	5Z	QZ−PP	2.300					
CCSD(T)			2.305					
MP2, ref 18		6-31G*	2.324					

[a] For details of basis sets, see computational section. [b] Difference of dimer terminal and monomer bond lengths. [c] Difference of bridging and terminal bond lengths.

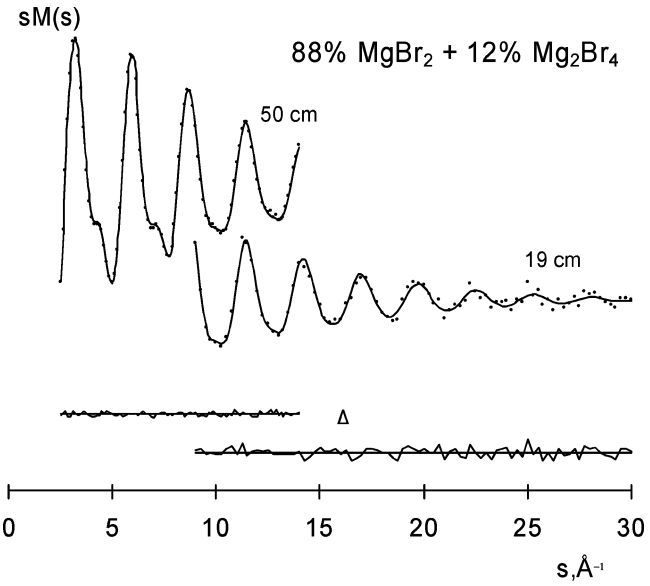

Figure 1. Experimental (dots) and calculated (solid line) molecular intensities and their differences (Δ) for magnesium dibromide at 1065 K.

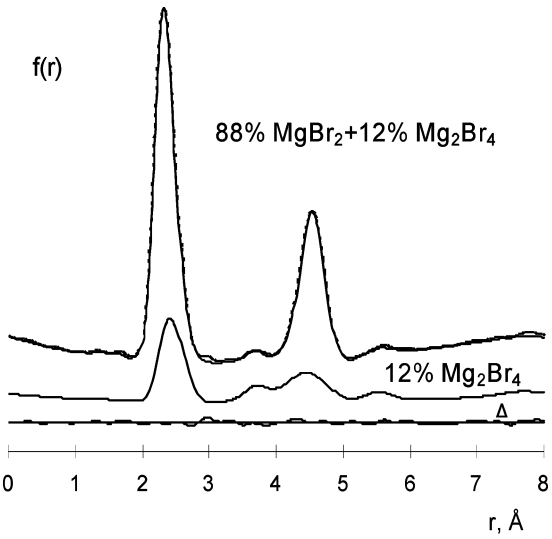

Figure 2. Experimental (dashed line) and calculated (solid line) radial distributions and their differences (Δ) for magnesium dibromide. The contribution of 12% of the dimeric molecules is also indicated.

a wide range of basis sets in order to get the best possible equilibrium geometry for the monomeric $MgBr_2$ molecule. Density functional (B3LYP), MP2 (full), and CCSD(T) methods were used with full geometry optimization. All computations were performed using the Gaussian03[23] program package. For magnesium, Dunning's all-electron basis sets were used, starting from triple-ζ quality up to quintuple-ζ with and without polarization functions.[24] Triple- and quadruple-ζ correlation-consistent polarized core/valence bases of Dunning et al.[25] were also tested (CTZ, CQZ). These sets include extra functions designed for core−core and core−valence correlation providing more accurate calculated parameters, such as shorter bond lengths. For bromine we tried all-electron basis sets[26] as well as pseudopotentials. Since relativistic effects are important for such a large atom as bromine, the Stuttgart-type relativistic effective core potentials (ECPs) of Bergner et al.,[27] covering 46 electrons, were eventually used; these latter incorporate scalar relativistic effects. The associated basis sets were of different types; triple- and quadruple-ζ correlation-consistent valence electron bases of Martin and Sundermann[28] (SDB−TZ, SDB−QZ) with and without diffuse functions. Fully relativistic, Dirac−Fock pseudopotentials were also tested with the correlation-consistent basis sets (TZ−PP, ATZ−PP, QZ−PP, AQZ−PP) of Peterson et al.[29] A set of the best computed geometrical parameters of the monomer $MgBr_2$ molecule together with those of the minimum-energy structure of the dimer are given in Table 1.

A recent study of some alkaline earth dihalide dimers showed that their minimum-energy structures may be different depending on whether their respective monomers are linear or bent. The dimers of linear monomers have D_{2h}, while those of the bent monomers have C_{3v} symmetry.[30] We have calculated dimer structures assuming these two symmetries in order to determine

TABLE 2: Geometrical Parameters of Different Isomers of Mg_2Br_4, Geometrical Parameters of the Mg_3Br_6 Molecule (distances in Å, angles in degrees), Number of Imaginary Frequencies (NIMAG), and Relative Energies (in kcal/mol) of the Dimers from Computation[a]

	Mg_1-Br_b	Mg_2-Br_b	Mg_1-Br_t	Mg_2-Br_t	$\angle Br_b-Mg_1-Br_b$	$\angle Br_b-Mg_2-Br_b$	NIMAG	ΔE
				Mg_2Br_4				
D_{2h} GS[b]	2.523	2.523	2.335	2.335	95.8	95.8	0	0.00
C_{3v}	2.731	2.452	2.344	-	86.6	99.6	0	14.28
C_s	2.619	2.487	2.338	2.379	90.3	96.5	1	15.37
				Mg_3Br_6				
D_{2d} GS[b]	2.536	2.519		2.337	95.7	96.5	0	-

[a] B3LYP/Mg:TZ (= cc−pvtz), Br:SDB−TZ, see computational section. [b] GS: ground-state structure.

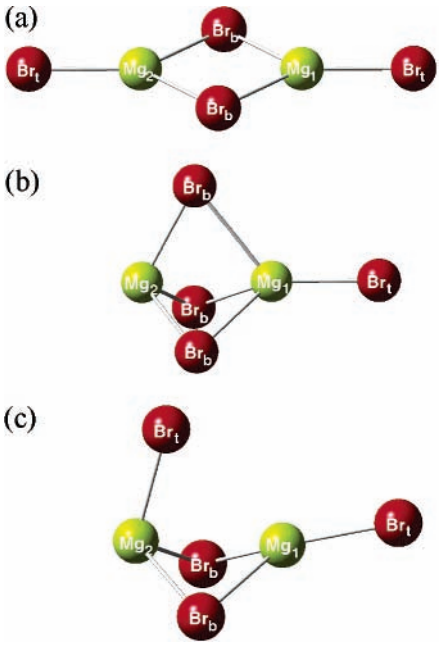

Figure 3. Molecular models of Mg_2Br_4: (a) model with D_{2h} symmetry (ground-state structure), (b) model with C_{3v} symmetry, and (c) model with C_s symmetry (transition-state structure).

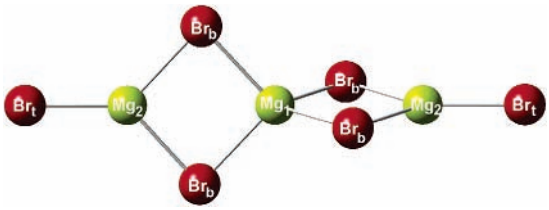

Figure 4. Molecular model and labeling of atoms in Mg_3Br_6.

their relative stabilities. The transition-state structure between them was also calculated; the geometrical parameters and relative energies of these structures are given in Table 2. The molecular models and labeling of atoms are shown in Figure 3. Two trimer structures were also examined, a D_{2d}-symmetry arrangement, found in an earlier study at the Hartree−Fock level,[18] and a D_{3h}-symmetry six-membered ring structure. The latter was found to be unstable. The geometrical parameters of the minimum-energy trimer structure are given in Table 2. The molecular model and the labeling of atoms are shown in Figure 4.

Computations determine the so-called equilibrium geometry, while electron diffraction measures thermal average geometries and their symmetry is often lower than that of the equilibrium structure. To see the effect of large-amplitude vibrations on the molecular geometry, we have computed the effect of puckering of the four-membered ring of the dimer molecule. We optimized all parameters of the dimer structure by changing the constant

TABLE 3: Ring Puckering Potential for Mg_2Br_4 from Computation (distances in Å, angles in degrees, energies in kcal/mol)[a]

Mg_1-X-Mg_2[b]	$Mg-Br_b$	$Mg-Br_t$	$Br_b-Mg-Br_b$	Br_t-Mg-X[c]	ΔE
0	2.523	2.336	95.8	180.	0.00
10	2.523	2.335	95.7	179.5	0.17
20	2.524	2.335	95.3	178.3	0.70
30	2.527	2.335	94.5	176.5	1.70
40	2.531	2.334	93.5	173.9	3.32
50	2.536	2.334	92.2	170.8	5.79
60	2.544	2.334	90.7	167.2	9.40

[a] B3LYP/Mg:TZ (= cc−pvtz), Br:SDB−TZ, see computational section. [b] Puckering angle of the Mg_2Br_2 ring. X is the midpoint of the $Br_b\cdots Br_b$ line. [c] Angle of the terminal Mg−Br bond and the $Br_b-Mg-Br_b$ plane.

TABLE 4: Vibrational Frequencies (cm^{-1}) of the $MgBr_2$ Monomeric Molecule from Computation and Experiment

method	basis set/Mg	basis set/Br	ν_1	ν_2	ν_3
MP2	ATZ	SDB−ATZ	198	94	531
MP2	ATZ	ATZ−PP	201	106	543
MP2	QZ	QZ	200	93	535
CCSD(T)	QZ	QZ	199	93	533
MP2	AQZ	SDB−AQZ	198	93	530
MP2	5Z	SDB−QZ	201	92	535
CCSD(T)	5Z	SDB−QZ	200	92	533
MP2	QZ	QZ−PP	201	103	540
CCSD(T)	QZ	QZ−PP	201	101	533
MP2	CQZ	AQZ−PP	201	106	540
MP2, ref 18			202.7	102.3	549.0
experimental, gas phase, ref 7					490
experimental, Ar matrix, ref 9			197.9	81.5	497.1
experimental, Ar matrix, ref 8					502, 509, 520
PC model[a] B3LYP	TZ	SDB−TZ	183	56	501

[a] Polarizable continuum model to model the Ar environment; see computational section.

puckering angles by 10° increments. The results are given in Table 3. It seems that during the puckering the terminal bond length of the dimer does not change, while the bridging bond length increases noticeably. The $Br_b-Mg-Br_b$ angle of the four-membered ring decreases, while the terminal bonds bend away from the original molecular plane and the molecule takes up a slightly pronounced W shape. The puckering motion of the ring is rather anharmonic, in that the energy of a 50° pucker is 34 times greater than that of the 10° pucker. Investigation of the puckering also made it possible to carry out a so-called dynamic electron diffraction analysis (vide infra).

Frequency calculations were also performed at different computational levels for the monomer, as shown in Table 4. The frequencies of the minimum-energy dimeric and trimeric molecules are given in Table 5. Most of the experimental frequencies of magnesium dibromide come from matrix isolation

TABLE 5: Computed Vibrational Frequencies (cm^{-1}) of Mg_2Br_4 and Mg_3Br_6 Molecules (IR intensities (km/mol) in square brackets)[a]

Mg_2Br_4				Mg_3Br_6	
D_{2h} (GS)[b]		C_{3v}		D_{2d}	
A_g	458.8	A_1	442.0 [83.7]	A_1	447.0
A_g	174.7	A_1	303.9 [78.5]	A_1	171.4
A_g	90.9	A_1	158.4 [8.9]	A_1	147.3
B_{2g}	97.5	A_1	120.2 [6.1]	A_1	60.1
B_{3g}	230.1	E	328.1 [88.9]	B_1	30.0
B_{3g}	62.3	E	126.6 [23.3]	B_2	446.8 [205.4]
B_{1u}	433.7 [275.3]	E	90.9 [0.4]	B_2	341.3 [255.6]
B_{1u}	154.4 [6.6]	E	47.0 [0.1]	B_2	166.9 [7.4]
B_{2u}	312.1 [110.8]			B_2	111.5 [1.5]
B_{2u}	41.6 [5.8]			E	310.7 [99.6]
B_{3u}	129.3 [43.1]			E	230.9 [<0.1]
B_{3u}	16.2 [2.4]			E	115.1 [18.8]
				E	67.3 [1.3]
				E	45.5 [1.4]
				E	11.4 [1.2]

[a] B3LYP/Mg:TZ (= cc−pvtz), Br:SDB−TZ, see computational section. [b] GS: ground-state structure.

experiments, therefore we tried to model the effect of the argon matrix using the so-called polarizable continuum model initially devised by Tomasi and co-workers[31] and implemented in Gaussian03 based on the work of Barone and co-workers[32] and Tomasi and co-workers.[33] These geometry optimizations were carried out at the B3LYP/Mg:TZ, Br:SDR−TX levels. The dimerization energy of $MgBr_2$ was also calculated at the MP2/Mg:QZ Br:QZ−PP levels, taking the BSSE correction into account.

Normal Coordinate Analysis. A normal coordinate analysis was performed based on the computed vibrational frequencies (MP2/QZ, QZ−PP) for both monomeric and dimeric $MgBr_2$ using the program ASYM20.[34] The mean-square vibrational amplitudes of the nonbonded distances in the dimer were especially useful for the electron diffraction analysis because due to the relatively small dimer content of the vapor it was expected that these amplitudes could not be refined in the analysis. According to the computations, the ground-state structure of the dimer has D_{2h} symmetry. This was the structure for which we carried out the normal coordinate analysis. The internal coordinates as well as the symmetry coordinates were the same as those chosen previously for Mg_2Cl_4.[11] The calculated vibrational amplitudes for both monomeric and dimeric molecules are given in the Supporting Information.

Electron Diffraction Analysis. Although the basic component of the vapor was the monomeric molecule, it was obvious from the mass spectra that there is a noticeable amount of dimer presence in the vapor. To reduce the strong correlation between closely spaced distances during the analysis, certain assumptions have been introduced. First of all, the difference between the monomer bond length and that of the dimer terminal bond was accepted from the computation. To use bond length *differences* from computation as constraints in the GED analysis is a generally accepted and justified approach. Even if the physical meaning of geometrical parameters from experiment and computation is not the same, these differences cancel to a good approximation if we use the *differences* of computed bond lengths rather than the bond lengths themselves as constraints in the GED analysis.[6,35] As Table 1 shows this difference was remarkably constant at different levels of computation. The variation of the difference of the monomer and the dimer terminal bond lengths is within 0.003 Å. The difference between the two dimer distances varies within 0.010 Å, but as it turned out, this parameter could be refined in the "static" structure analysis.

The structure analysis was carried out in two different ways. One of them was the traditional "static" analysis, the other the so-called "dynamic analysis". In the first case, one "static" structure describes the molecular geometry, whose symmetry, however, is lower than that of the equilibrium structure. The symmetry lowering is due to the thermal average nature of the GED geometries and to the large amplitude deformation vibrations of the molecules.[6,35] In this case, even if $MgBr_2$ has a linear and Mg_2Br_4 a D_{2h}-symmetry planar equilibrium geometry, they appear as bent and puckered, respectively. In this analysis, only the difference of the monomer and dimer terminal bond lengths was constrained at the computed value; all other geometrical parameters could be refined. The only other constraint we applied in this analysis was the grouping of the vibrational amplitudes of closely spaced distances (mostly those of the dimer) and also the grouping of the asymmetry parameters of the three Mg−Br distances.

The "dynamic" analysis uses a set of "conformers" in order to approximate the thermal average nature of the experimental structures. On the basis of our earlier experience,[36] we used the computed conformer structures only for the dimer molecule. These dimer "conformers" are the geometries that were computed for gradually changing puckering angles; see Table 3. In this analysis, the relative contributions of the different "conformers" were estimated from their relative energies by the expression $V = \exp(-\Delta E/RT)$. To describe the contribution of these different conformers, again, only parameter differences were taken over from the computation to the electron diffraction analysis.

As is usually the case in high-temperature electron diffraction studies of metal halides, the anharmonicity of the stretching vibrations, described by the so-called asymmetry parameter (κ), could not be ignored. The starting value of this parameter was estimated by the expression $\kappa = a l_T^4(3 - 2l_0^4 l_T^{-4})/6$, where a is the Morse parameter, l_T is the mean-square vibrational amplitude at the temperature of the experiment, and l_0 is the mean-square vibrational amplitude at 0 K.[37,38] Initially the Morse parameter was chosen to be 1.5 $Å^{-1}$ based on our experience with similar metal dihalides.[38] The asymmetry parameters of the three different Mg−Br distances were then refined in a group. The asymmetry parameter obtained this way corresponds to a Morse parameter $a = 1.65$ $Å^{-1}$, which is a realistic value. The results of the GED analyses are given in Table 6.

Results and Discussion

The bond length of the monomer $MgBr_2$ molecule was calculated at a wide range of method/basis set combinations (see Table 1). Most of them give a bond length between 2.32 and 2.33 Å and that agrees with the previously determined values by Axten et al.,[18] but these values are more than 0.01 Å longer than the estimated experimental equilibrium distance. It is only the quadruple-ζ bases on Mg with the fully relativistic Dirac−Fock pseudopotentials and large quadruple-ζ valence basis sets on Br that give bond lengths around 2.310 Å that are close to the estimated equilibrium bond length from electron diffraction, 2.307(8) Å. The inclusion of diffuse functions (on either or both types of atoms) very slightly lengthens the bonds, but the effect is marginal. The bond length is a few thousandths of an angstrom larger from the CCSD(T) computation than that from the MP2 (full) with the same basis sets. If we accept the generally observed fact that the MP2 method somewhat underestimates bond lengths, then the CCSD(T) computations

TABLE 6: Geometrical Parameters of $MgBr_2$ and Mg_2Br_4 from Electron Diffraction[a]

	static model	dynamic model
	$MgBr_2$	
r_g(Mg−Br)	2.325 ± 0.006	2.326 ± 0.006
r_e^M(Mg−Br)[b]	2.307 ± 0.008	2.308 ± 0.008
l(Mg−Br)	0.086 ± 0.003	0.085 ± 0.003
κ(Mg−Br)	$4.3\times 10^{-5} \pm 1.4 \times 10^{-5}$	$4.3\times 10^{-5} \pm 1.4 \times 10^{-5}$
r_g(Br···Br)	4.550 ± 0.010	4.548 ± 0.010
l(Br···Br)	0.143 ± 0.005	0.143 ± 0.005
δ_g(Br···Br)	0.100 ± 0.008	0.104 ± 0.008
	Mg_2Br_4[c]	
r_g(Mg−Br_t)	2.333 ± 0.007	2.335 ± 0.007
l(Mg−Br_t)	0.084[d]	0.083[d]
κ(Mg−Br_t)[e]	4.2×10^{-5}	4.0×10^{-5}
r_g(Mg−Br_b)	2.523 ± 0.015	2.528 ± 0.008
l(Mg−Br_b)	0.126[d]	0.139[d]
κ(Mg−Br_b)[e]	1.9×10^{-4}	1.9×10^{-4}
$\Delta(D_t - \text{Mon})$	[0.008][f]	[0.009][g]
$\Delta(D_b - D_t)$	0.190 ± 0.014	[0.193][g]
$\angle Br_b$−Mg−Br_b	94.8 ± 0.9	[95.8][g]
$\angle_\alpha$,[h]	35.3 ± 4.9	
Dimer (%)	12.1 ± 1.5	12.7 ± 1.5
R (%)[i]	7.2	7.6

[a] Bond lengths (r_g), vibrational amplitudes (l), and shrinkage (δ_g) in Å, angles in degrees, and asymmetry parameters (κ) in Å^3. Error limits are estimated total errors, including systematic errors and the effect of constraints used in the refinement: $\sigma_t = (2\sigma_{LS}^2 + (cp)^2 + \Delta^2)^{1/2}$, where σ_{LS} is the standard deviation of the least squares refinement, p is the parameter, c is 0.002 for distances and 0.02 for amplitudes, and Δ is the effect of constraints. [b] Estimated (by anharmonic corrections) experimental equilibrium distance. [c] For molecular model and numbering of atoms, see Figure 3a. [d] Refined together with the monomer amplitude. [e] Refined together with the monomer asymmetry parameter. [f] Constrained at the computed value at the MP2/Mg:QZ, Br:QZ−PP level. [g] Constrained at the computed values at the B3LYP/Mg:TZ, Br: SDB−TZ level. [h] Puckering of the four-membered central ring of the dimer. [i] Goodness of fit.

with fully relativistic ECP and the QZ−PP valence basis on Br and high-level basis sets on Mg give the best results. Interestingly, with the above ECP/basis set combination on Br, the change of the Mg basis from QZ to CQZ and then to 5Z further decreases the Mg−Br bond length by 0.004 and then by 0.005 Å, respectively, the latter value being already smaller than the estimated experimental equilibrium bond length.

For the dimer computations the highest level we used was the MP2/Mg:QZ, Br/QZ−PP. This is the set of data from which we accepted the monomer and dimer terminal bond length differences. However, this difference was fairly constant at all levels of the computation.

The minimum-energy structure of the dimer is the D_{2h}-symmetry arrangement (see Figure 3). The C_{3v}-symmetry structure with three halogen bridges is also a local minimum with all positive frequencies, but it lies about 14 kcal/mol higher in energy than the global minimum D_{2h}-symmetry structure. We have also calculated the transition-state structure (one imaginary frequency) between these two arrangements. It has C_s symmetry (see Figure 3) and lies barely about 1 kcal/mol higher in energy than the C_{3v}-symmetry structure.

The details of the trimer structure are similar to that of the dimer, except the central part; the bonds of the four-coordinated magnesium atom, Mg_1−Br_b, are about 0.01 Å longer than the other bridging bonds that are connected with three-coordinated magnesium atoms (see Table 2 and Figure 4). The latter as well as the terminal Mg−Br_t bonds are of about the same length as those in the dimer.

The computed vibrational frequencies of the monomer are given in Table 4 together with the experimental values and previous computational result; for the latter, only the ones calculated at higher than HF level are given. There is only one experimental gas-phase frequency available from the literature, viz., the ν_3 asymmetric stretching frequency.[7] All monomer frequencies and some of those of the dimer measured in the argon matrix have been reported by Lesiecki and Nibler.[9] There is also another argon-matrix IR work by Cocke et al. in the literature that reports three bands at 502, 509, and 520 cm^{-1} that can be assigned to the asymmetric stretching frequency.[8]

The computed symmetric stretching frequency is only a few cm^{-1} higher than the argon-matrix value from ref 9, which is reasonable. The situation with the asymmetric stretching frequency is more difficult. It is hard to judge the reliability of the reported experimental asymmetric stretching frequencies. The work reporting the gas-phase frequency is a barely half-page note that does not show the actual spectrum.[7] The reported frequency, 490 cm^{-1}, agrees well with the one reported in one of the argon-matrix works,[9] 497 cm^{-1}; alas one would expect a larger value in the gas phase than in the matrix, in which, due to the inevitable interaction with the matrix sites, one would expect a weakening of the bond. At the same time, there is a disagreement between the two argon-matrix studies concerning this frequency, and this discrepancy is not commented on in the relevant papers. The computed asymmetric stretching frequency is considerably higher than either of the experimental ones, even from the best computations (between 530 and 540 cm^{-1}, about 20−40 cm^{-1} higher than the experimental values). The agreement between experiment and computation is also poor for the bending frequency; the computed values being about 10−20 cm^{-1} larger than the experimental ones.

There are several possible reasons for such discrepancies. There are two obvious ones; one of them pertains to the possibility of matrix effects in the experiment. Our trial calculations with the polarizable continuum model of Tomasi et al.,[31] in which we put the $MgBr_2$ molecule into an "argon solvent", showed quite a large change in the frequencies of $MgBr_2$; the asymmetric stretching frequency (501 cm^{-1}) decreased noticeably compared with the calculated value for the free $MgBr_2$ molecule and is much closer to the experimental argon-matrix frequencies. The symmetric stretching frequency does not change that much, but the bending frequency becomes much smaller than either the experimental or the gas-phase value. Naturally, these calculations are only very approximate, but at least they indicate that the effect of the matrix is definitely a factor in the experiment.

Another reason for the disagreement between computed and experimental frequencies could be that while computations provide harmonic frequencies, the experimental values are probably anharmonic, considering the high temperatures of evaporation. It is difficult to judge the effect of anharmonicity, but based on recent results on lanthanide trihalides, the anharmonicity of these vibrations may be considerable and is of the opposite sign for the stretching and for the out-of-plane vibration. As discussed by Lanza and Minichino,[39] the stretching frequencies decrease due to the anharmonicity, while the puckering out-of-plane frequency substantially increases. If it is possible to draw conclusions from this for alkaline earth dihalides, these two effects would bring the computed and experimental asymmetric stretching frequencies closer to each other and would more or less cancel out for the bending frequencies. Of course, we have to consider that the lower the frequency, the larger the difficulties we encounter with the computations. Therefore, this situation cannot be considered as resolved yet; new vibrational experiments would be needed for that.

We have also calculated the vibrational frequencies of the dimeric and trimeric molecules; they are given in Table 5. This is the first computation of the trimer frequencies; the ones for the dimer agree reasonably well with the ones calculated earlier at the Hartree−Fock level[18] and also with the suggested few wavenumbers from the argon-matrix experiment.[9]

The thermal average bond length, r_g, of the monomeric $MgBr_2$ molecule from electron diffraction is 2.325(6) Å. When vibrational corrections were applied to this value, the experimental equilibrium bond distance was estimated to be 2.307(8) Å in good agreement with the results of the best computations. The asymmetry parameter of the Mg−Br bond length was also determined, even if with a rather large uncertainty. It is difficult to determine this parameter. First of all, it is sensitive to the larger scattering-angle region of the molecular intensity curve, which has a large noise due to the experimental conditions. At the same time, this parameter strongly correlates with the dimer content. To overcome this problem, we decided first to estimate the dimer content from the 50 cm experimental curve, assuming zero value for the asymmetry parameter. This is a reasonable assumption, since the asymmetry parameter does not have a noticeable effect on the small-scattering region while the dimer content (due to the larger contribution of the longer nonbonded distances) dominates this region.

Our electron diffraction analysis showed about 12% dimers in the vapor phase under the experimental conditions. This is in accordance with our quadruple mass spectrometric studies, which also indicated a considerable presence of dimeric species; from the ions originating from the dimer, the $Mg_2Br_5^+$ ion was the most intense, but other ions, such as $Mg_2Br_2^+$ and Mg_2Br^+, could also be detected. An earlier mass spectrometric study of the magnesium dihalides indicated only about a 1% dimer content for each halide.[12] However, the GED experiment of magnesium dibromide was performed at about 250° higher temperature than that of the mass spectrometric experiment.[12] As the slope of the partial pressure (the logarithm of the ion intensity ratio) vs reciprocal temperature plot of the dimer is steeper than that of the monomer, the relative amount of dimers in the vapor increase as the temperature increases. Extrapolation of the vapor pressure data from ref 12 to our experimental temperature shows that at our experimental conditions we can expect the dimer content to be larger by an order of magnitude and this agrees with our findings. This is in agreement with the so-called Brewer's rule.[40]

We have also computed the dimerization energy of magnesium dibromide. The BSSE correction is rather large, about 6 kcal/mol. The BSSE corrected standard dimerization enthalpy, $\Delta H° = -34.8$ kcal/mol, is in remarkably good agreement with the value −32 kcal/mol, estimated from simple relationships and atomization energies.[41]

Acknowledgment. We thank Dr. Dezsö Knausz for the preparation of the anhydrous magnesium dibromide sample. We are grateful to the Hungarian National Research Fund (OTKA T 037978) for financial support.

Supporting Information Available: Electron diffraction molecular intensities at two different camera ranges and calculated vibrational amplitudes for $MgBr_2$ and Mg_2Br_4. This material is available free of charge via the Internet at http://pubs.acs.org.

References and Notes

(1) Grignard, V. C. R. *Hebd. Seances Acad. Sci*. **1900**, *130*, 1322.
(2) Schlenk, W.; Schlenk, W., Jr. *Chem. Ber*. **1929**, *62*, 920.
(3) Wells, A. F. *Structural Inorganic Chemistry*, 4th ed.; Clarendon Press: Oxford, U.K., 1975.
(4) Schneider, M.; Kuske, P.; Lutz, H. D. *Acta Crystallogr*. **1992**, *B48*, 761.
(5) For a summary and references, see, Spiridonov, V. P. *Kém. Közl.* **1972**, *37*, 399.
(6) Hargittai, M. *Chem. Rev*. **2000**, *100*, 2233.
(7) Randall, S. P.; Green, F. T.; Margrave, J. L. *J. Phys. Chem.* **1959**, *63*, 758.
(8) Cocke, D. L.; Chang, C. A.; Gingerich, K. A. *Appl. Spectrosc.* **1973**, *27* (4), 260.
(9) Lesiecki, M. L.; Nibler, J. W. *J. Chem. Phys.* **1976**, *64* (2), 871.
(10) For references see, e.g., ref 6 and Hargittai, M. *Coord. Chem. Rev.* **1988**, *91*, 35.
(11) Molnár, J.; Marsden, C. J.; Hargittai, M. J. *Phys. Chem*. **1995**, *99*, 9062.
(12) Berkowitz, J.; Marquart, J. R. *J. Chem. Phys*. **1962**, *37*, 1853.
(13) Vajda, E.; Hargittai, M.; Hargittai, I.; Tremmel, J.; Brunvoll, J. *Inorg. Chem.* **1987**, *26*, 1171.
(14) Hargittai, M.; Kolonits, M.; Knausz, D.; Hargittai, I. *J. Chem. Phys.* **1992**, *96*, 8980.
(15) Hargittai, M.; Kolonits, M.; Schultz, Gy. *J. Mol. Struct*. **2001**, *567−568*, 241.
(16) Seijo, L.; Barandiarán, Z. *J. Chem. Phys.* **1991**, *94* (5), 3762.
(17) Knaupp, M.; Schleyer, P. v. R.; Stoll, H.; Preuss, H. *J. Am. Chem. Soc.* **1991**, *113*, 6012.
(18) Axten, J.; Trachtman, M.; Bock, C. W. *J. Phys. Chem.* **1994**, *98*, 7823.
(19) Brauer, G. *Handbook of Preparative Inorganic Chemistry*; Academic Press: New York, 1963; pp 909−910.
(20) Hargittai, I.; Tremmel, J.; Kolonits, M. *Hung. Sci. Instrum*. **1980**, *50*, 31. Hargittai, I.; Bohatka, S.; Tremmel, J.; Berecz, I. *Hung. Sci. Instrum.* **1980**, *50*, 51−56.
(21) Tremmel, J.; Hargittai, I. *J. Phys. E* **1985**, *18*, 148.
(22) Ross, A. W.; Fink, M.; Hilderbrandt, R.; Wang, J.; Smith, V. H., Jr. In *International Tables for Crystallography*, *C*; Wilson, A. J. C., Ed.; Kluwer: Dordrecht, Holland, 1995; pp 245−338.
(23) Frisch, M. J.; Trucks, G. W.; Schlegel, H. B.; Scuseria, G. E.; Robb, M. A.; Cheeseman, J. R.; Montgomery, J. A., Jr.; Vreven, T.; Kudin, K. N.; Burant, J. C.; Millam, J. M.; Iyengar, S. S.; Tomasi, J.; Barone, V.; Mennucci, B.; Cossi, M.; Scalmani, G.; Rega, N.; Petersson, G. A.; Nakatsuji, H.; Hada, M.; Ehara, M.; Toyota, K.; Fukuda, R.; Hasegawa, J.; Ishida, M.; Nakajima, T.; Honda, Y.; Kitao, O.; Nakai, H.; Klene, M.; Li, X.; Knox, J. E.; Hratchian, H. P.; Cross, J. B.; Bakken, V.; Adamo, C.; Jaramillo, J.; Gomperts, R.; Stratmann, R. E.; Yazyev, O.; Austin, A. J.; Cammi, R.; Pomelli, C.; Ochterski, J. W.; Ayala, P. Y.; Morokuma, K.; Voth, G. A.; Salvador, P.; Dannenberg, J. J.; Zakrzewski, V. G.; Dapprich, S.; Daniels, A. D.; Strain, M. C.; Farkas, O.; Malick, D. K.; Rabuck, A. D.; Raghavachari, K.; Foresman, J. B.; Ortiz, J. V.; Cui, Q.; Baboul, A. G.; Clifford, S.; Cioslowski, J.; Stefanov, B. B.; Liu, G.; Liashenko, A.; Piskorz, P.; Komaromi, I.; Martin, R. L.; Fox, D. J.; Keith, T.; Al-Laham, M. A.; Peng, C. Y.; Nanayakkara, A.; Challacombe, M.; Gill, P. M. W.; Johnson, B.; Chen, W.; Wong, M. W.; Gonzalez, C.; Pople, J. A. *Gaussian 03*, revision B.05; Gaussian, Inc.: Pittsburgh, PA, 2003.
(24) (a) Kendall, R. A.; Dunning, T. H., Jr.; Harrison, R. J. *J. Chem. Phys.* **1992**, *96*, 6796. (b) Dunning, T. H., Jr. *J. Chem. Phys.* **1989**, *90*, 1007. (c) Peterson, K. A.; Woon, D. E.; Dunning, T. H., Jr. *J. Chem. Phys.* **1994**, *100*, 7410.
(25) Woon, D. E.; Peterson, K. A.; Dunning, T. H., Jr. To be submitted for publication.
(26) Woon, D. E.; Dunning, T. H., Jr. To be submitted for publication.
(27) Bergner, A.; Dolg, M.; Kuechle, W.; Stoll, H.; Preuss, H. *Mol. Phys.* **1993**, *80*, 1431.
(28) Martin, J. M. L.; Sundermann, A. *J. Chem. Phys.* **2001**, *114*, 3408.
(29) Peterson, K. A.; Figgen, D.; Goll, E.; Stoll, H.; Dolg, M. *J. Chem. Phys*. **2003**, *119*, 11113.
(30) Levy, J. B.; Hargittai, M. *J. Phys. Chem. A* **2000**, *104*, 1950.
(31) Tomasi, J.; Mennucci, B.; Cancès, E. *J. Mol. Struct. (THEOCHEM)* **1999**, *464*, 211.
(32) Cossi, M.; Scalmani, G.; Rega, N.; Barone, V. *J. Chem. Phys.* **2002**, *117*, 43.
(33) Cammi, R.; Mennucci, B.; Tomasi, J. *J. Phys. Chem. A* **2000**, *104*, 5631.
(34) Hedberg, L.; Mills, I. M. *J. Mol. Spectrosc*. **1993**, *160*, 117.
(35) Hargittai, M.; Hargittai, I. *Int. J. Quantum Chem*. **1992**, *44*, 1057.
(36) Réffy, B.; Marsden, C. J.; Hargittai, M. *J. Phys. Chem. A* **2003**, *107*, 1840.
(37) Kuchitsu, K. *Bull. Chem. Soc. Jpn.* **1967**, *40*, 505.
(38) Hargittai, M.; Subbotina, N. Y.; Kolonits, M.; Gershikov, A. G. *J. Chem. Phys.* **1991**, *94*, 7278.
(39) Lanza, G.; Minichino, C. *J. Phys. Chem. A* **2004**, *108*, 4949.
(40) Lewis, G. N.; Randall, M.; Pitzer, K. S.; Brewer, L. *Thermodynamics*, 2nd ed.; McGraw-Hill: New York, 1961; Chapter 33.
(41) Hargittai, M.; Jancsó, G. *Z. Naturforsch*. **1993**, *48a*, 1000.